Supporting Material

Kinetics of the Multi-Step Rupture of Fibrin 'A-a' Polymerization Interactions Measured using AFM

Laurel E. Averett, Mark H. Schoenfisch, Boris B. Akhremitchev, and Oleg V. Gorkun

SUPPORTING MATERIAL

Kinetics of the Multi-Step Rupture of Fibrin 'A-a' Polymerization Interactions Measured using AFM

Laurel E. Averett, Mark H. Schoenfisch, Boris B. Akhremitchev, Oleg V. Gorkun

Data analysis and filtering

To determine which force curves to include in final analysis, the data set was filtered both manually and automatically. The data set was first analyzed with an automatic filter to identify force curves that included an interaction between the molecules on the tip and the substrate. In these experiments, an interaction was defined by the appearance of a rupture event (i.e. a sudden relaxation of pulling force with change greater than 5 times the standard deviation of the baseline noise). Such events were required to occur with a tip-substrate separation between 10 to 200 nm. These limits were chosen based on the length of fibrinogen (45 nm). Of note, extending this range did not change the force probability distributions. Based on this filter, 48% of force curves collected contained a rupture event and therefore an interaction between the molecules on the tip and substrate.

To be considered for analysis, the force curves had to contain the characteristic pattern of bond rupture. The criteria defining this pattern, which were established empirically, were: each curve had to possess two consecutive events (i.e., a doublet) with magnitudes differing by less than 50 pN. A preceding event of any magnitude and/or a following event more than 75 pN less than the magnitude of the first event of the doublet was also acceptable. The filter criteria were optimized to include the expected low-force tails in the force probability distributions and to restrict scatter in the force versus relative separation plots, eliminating ~ 56% of curves exhibiting some rupture events.

The remaining curves were subjected to a secondary manual filter to eliminate non-characteristic force curves. Since the automatic filter did not include requirements for relative separations, some of the curves identified as characteristic had uncharacteristically large relative separations (> 30 nm) between events. Such curves represented < 20% of the remaining force curves and were identified and eliminated by hand. Examples of curves eliminated by both the automatic and manual filters are given below (Fig. S1). The number of curves analyzed herein was 6555.

As all interactions, both excluded and included in analysis, were able to be eliminated using competitive inhibition of the 'A-a' interaction (13), the excluded curves likely represent heterogeneity in the rupture of the 'A-a' bond and will be a subject for future examination. Heterogeneity in the 'A-a' interaction is most likely due to differences in orientation of the surface-bound protein; indeed, pull direction has been shown to be a significant parameter in forced protein unfolding (19, 20).

After selection, the force curves were divided into four types: curves with just the doublet (type A), curves with the doublet and a preceding event (type B), curves with the doublet and a following event (type C), and curves with all four events (type D) (Fig. 2). No analyses performed herein found that the behavior of any of the rupture events were dependent on force curve type. Therefore, the data presented represents the average behavior, weighted by the standard deviation. The force and tip-surface separation at rupture, and loading rate of each event were extracted from the data and used for subsequent analysis. The loading rate was

approximated from the slope of a line just prior to each event in the force curve (dashed line in Fig. 2).

**TABLE S1: Kuhn length (nm) of each event**

Model	Event 1	Event 2	Event 3	Event 4
Par	1.5 ± 1	0.19 ± 0.03	0.20 ± 0.02	0.30 ± 0.06
Ser	0.11 ± 0.03	0.18 ± 0.03	0.19 ± 0.02	0.30 ± 0.05

Kuhn lengths obtained from fitting the force curves with the freely-jointed chain (FJC) model with events 1 and 2 in parallel (Par) and series (Ser). Values represent averages of all curve types, weighted by the associated standard deviation. Errors represent the propagated standard deviation of each fitted parameter over n > 1000 force curves.
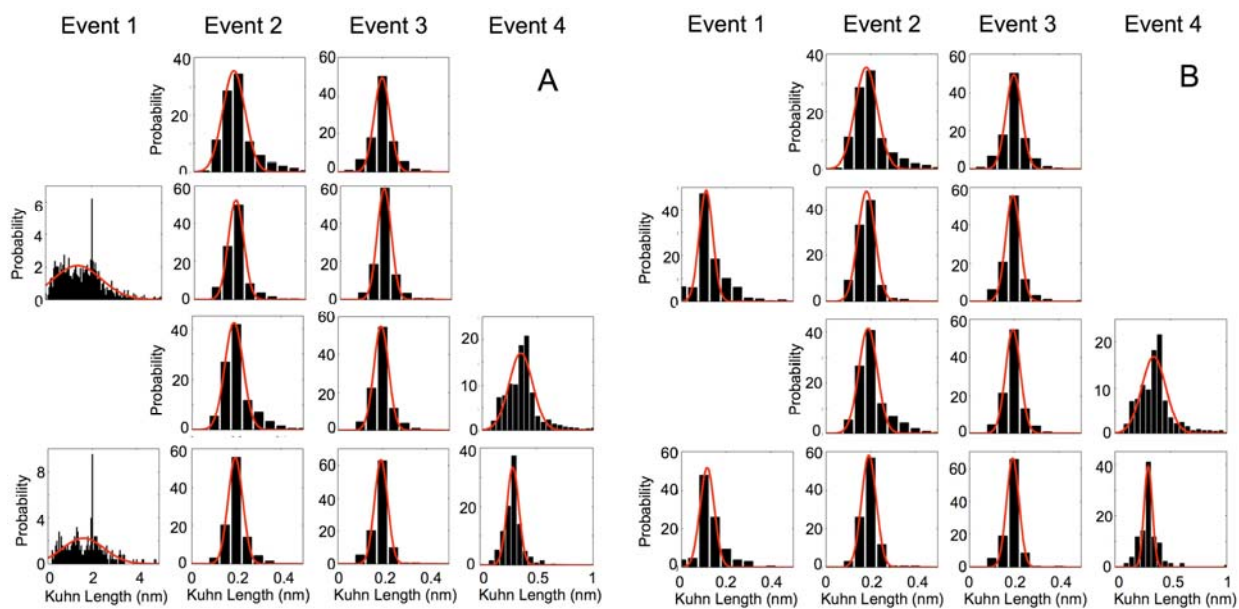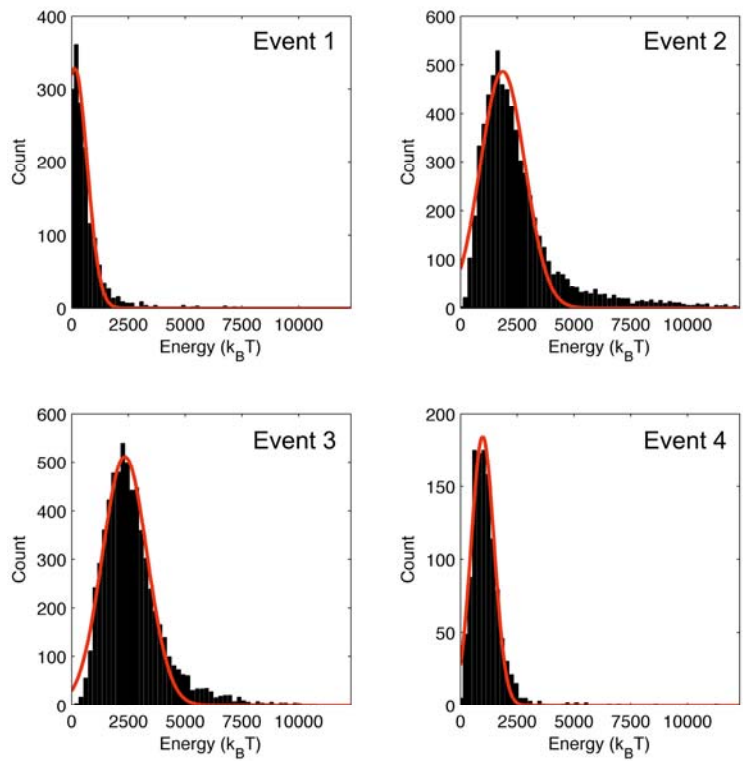
FIGURES
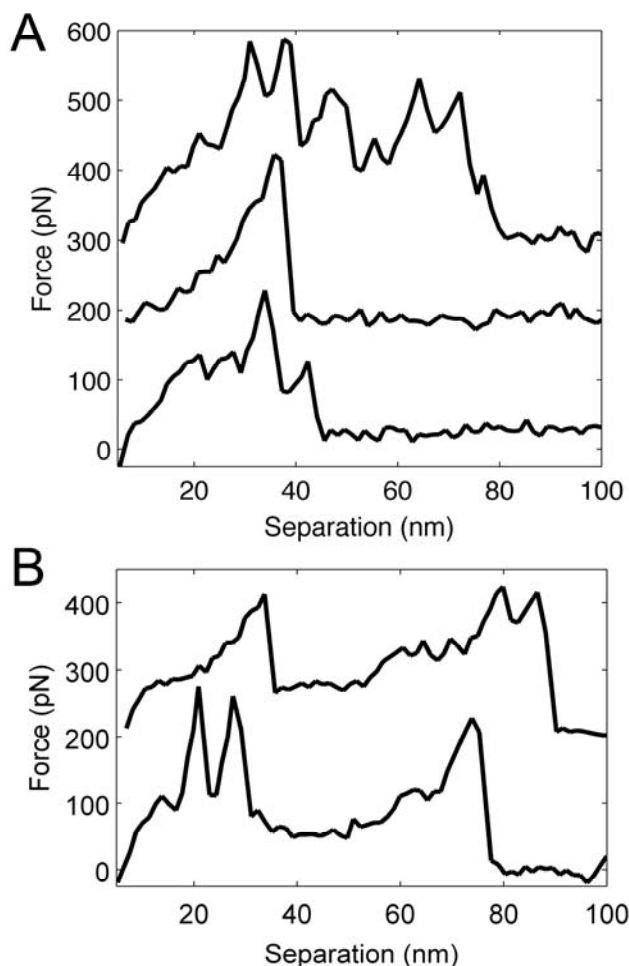
SUPPORTING MATERIAL FIGURE 1 Representative force curves not containing the characteristic pattern that were eliminated (*A*) automatically and (*B*) manually as described above. The automatic filter excludes curves with an overabundance of events (top), single events (middle), and curves that don't fit the above definitions (bottom). The manual filter identified non-characteristic curves that passed the automatic filter but had events that were too far apart to be characteristic. These often include a doublet of events.
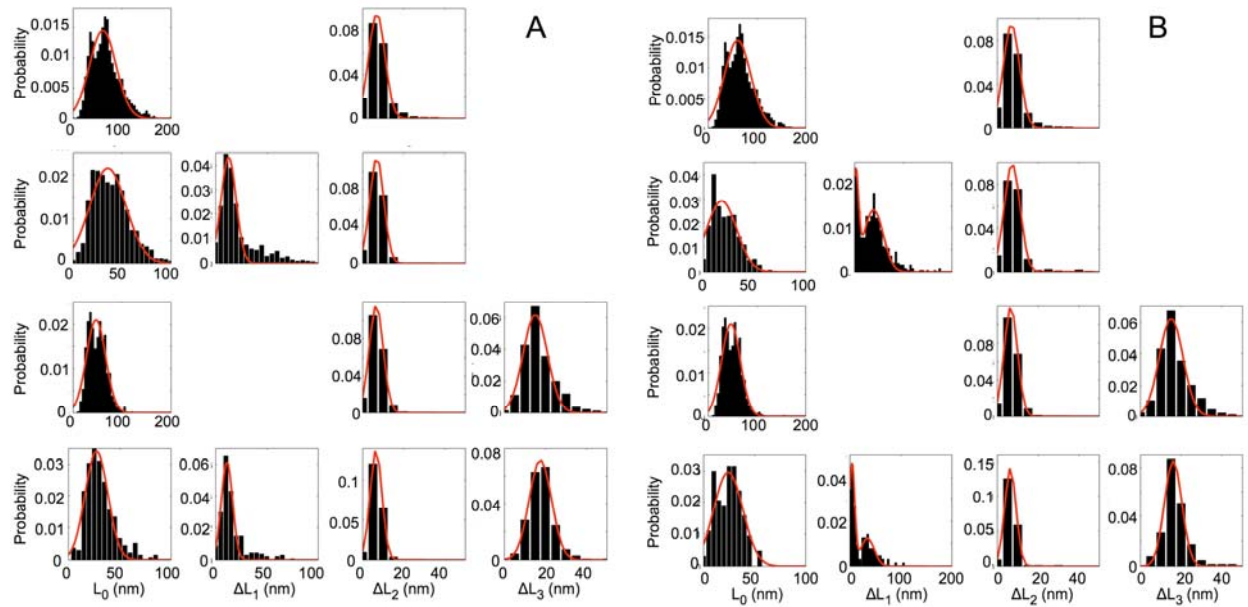
SUPPORTING MATERIAL FIGURE 2 Probability distributions and Gaussian fits of the initial contour length and increases in contour length for each event in each curve type as modeled with events 1 and 2 in (*A*) parallel and (*B*) series. Bin size = 5 nm. Each row corresponds to a curve type: curves with events 2 – 3 (*top row*), curves with events 1 – 3 (*second row*), curves with events 2 – 4 (*third row*), and curves with all four events (*last row*). Since there were not large differences in the increase in contour length based on curve type, the values presented in Table 1 represent the averaged position and standard deviation of each fit for the increases in contour length after each event, weighted by the standard deviation. Note that the change in contour length after event 1 has a narrower distribution when events 1 and 2 are in parallel, similar to the results in Figure 6. The initial contour length of the curves tends to be broad, and sometimes has two populations. This is attributable to the ensemble of orientations in which the protein is immobilized. Since they don't represent an identifiable pattern, the initial contour lengths are omitted from Table 1 and the main body of the manuscript.

SUPPORTING MATERIAL FIGURE 3 Probability distributions and Gaussian fits of Kuhn length for each event in each curve type as modeled with events 1 and 2 in (*A*) parallel and (*B*) series. Bin size = 0.05 nm. Each row corresponds to a curve type; the curve type corresponds to the events included in that row (e.g., the top row includes all curves that just exhibited events 2 and 3). Since there were no large differences in the values gained for each curve type, the values presented in Supplemental Material Table 1 represent the averaged position and standard deviation of each fit for the Kuhn length of each event, weighted by the standard deviation.

SUPPORTING MATERIAL FIGURE 4 Probability distributions and Gaussian fits of the elastic energy stored the protein at time of rupture. The fit values for each event are – event 1: $130 \pm 770\ k_BT$; event 2: $1850 \pm 1390\ k_BT$; event 3: $2340 \pm 1390\ k_BT$; event 4: $970 \pm 710\ k_BT$.